Responses to Editorial comments.

One referee still has critical concern on your method for quantification of local and non-local source contribution to ozone in TP, which I agree. I think that the QNR result should be considered as semi-quantitative given it has not considered non-linear ozone chemistry. As other parts of your analysis including trend results and the role of meteorology by GEOS-Chem are sound, I suggest you tone down the conclusion drawn from the QNR analysis, and add more clarification on the choice of QNR (in the method section), such as lack of high-resolution anthropogenic emission inventories in TP, thus hindering the use of a CTM in assessing local and non-local source contributions, and elaborate QNR limitations and suggest ways to improve the source attribution result (in the conclusion section).

Reply: We thank the editor for further comments. Indeed, the QNR method has its limitations by simplification of the ozone chemistry and the role of VOC emissions. In the revised manuscript, we have added nested GEOS-Chem CTM simulations to analyze the impacts of VOC emission changes and the nonlinearity in ozone chemistry. We have also added necessary discussion on the limitations of our method. Furthermore, we have further improved the PHLET-OMI NO_x emissions, which has a minor impact on our ozone change attribution. Please see details below and in our revised manuscript.

Responses to Referee 2's comments

In this study, the authors did not use the CTM to quantify the contribution of non-local factors on ozone issues in TP but the HYSPLIT (the QNR method), quoting that there were large uncertainties for the VOCs (line 305-306). However, the QNR method also had uncertainties due to the fact it did not consider the nonlinearity in ozone formation chemistry (line 179). So how the authors justify their choices of one method over another? At least by using the CTM, the comparisons will be consistent.

Reply: Thank you for your suggestion that the QNR method cannot account for the nonlinearity in ozone formation chemistry, which introduces uncertainty. To validate the QNR results and the effect of the nonlinearity in ozone formation chemistry, we have added high-resolution CTM simulations. The model configuration, results and discussion have been added to the main text and supplementary material.

Lines 420-437:

"Given the limitations of the QNR method in not accounting for VOC emissions and chemical nonlinearity, we further conduct nested GEOS-Chem simulations for summer (June, July and August) 2015 and 2019 to compare with the QNR results. The model is driven by our updated anthropogenic NO_x emissions as well as rough adjustments of anthropogenic VOC emissions over the TP based on current literature, including enhancement of VOC emissions upon the current inventories and emission growth in recent years (Supplementary material S1). To focus on the impact of chemistry, the meteorology is fixed at the 2015 level, but the anthropogenic emissions are adjusted in different model simulation scenarios (Table S1). The GEOS-Chem results show that when changes of NO_x and VOC emissions were considered together, increases in local and non-local emissions from 2015 to 2019 increase the summertime ozone in the TP cities by comparable amounts (0.71 ppb versus 1.21 ppb averaged over 17

cities), and inclusion of local and non-local emissions together lead to an larger ozone increase (1.52 ppb) (Table S2). Increases in NO_x emissions are the main driver of the simulated ozone growth ─ the ozone increase caused by NO_x emission increase alone is close to when both NO_x and VOC emission increases are taken into account (1.34 ppb versus 1.52 ppb when local and non-local emission changes are considered together, and 1.02 ppb versus 1.21 ppb when non-local emission changes are considered alone). These model results suggest that the ozone nonlinearity and the changes in anthropogenic VOC emissions have relatively small effects on the TP urban ozone growth studied here, and the use of QNR leads to reliable inference regarding the local and non-local drivers of TP ozone growth. Nevertheless, the nested GEOS-Chem simulations still underestimate the observed ozone growth in the TP cities, which are likely due to the lack of reliable high-resolution VOC emission information (including the simplicity in our VOC emission adjustments), the small spatial domain of TP cities, and the complex topography, as detailed in Section 2.3."

Supplementary material S1:

"We use nested GEOS-Chem simulations over Asia (60°E – 150°E, -11°N – 55°N) at the native resolution of 0.5° lat. × 0.625° long. to simulate the summertime (June, July and August) ozone change from 2015 to 2019. All nested simulations obtain the boundary conditions of chemicals from the global simulations at 2° lat. × 2.5° long. for the corresponding year. The global and nested simulations are run 6 months and 6 days in advance, respectively, as model spin-up to remove the impact of initial conditions. Compared to the global model setup in Section 2.3, the nested simulations only adjust the NO_x and NMVOC emissions, leaving the rest of the model settings unchanged. To focus on the impacts of emissions and chemical nonlinearity, the meteorological variables to drive the nested model simulations are fixed at the 2015 levels.

For anthropogenic NO_x emissions, we use the emission data in Section 2.4. For anthropogenic VOC emissions, we use the CEDS inventory globally, but used the MEIC (Multi-scale Emissions Inventory of China; www.meicmodel.org) v1.4 inventory (Li et al., 2017; Zheng et al., 2018) for China for VOC species available in MEIC (including acetone, acetaldehyde, lumped C4 + C5 alkanes, ethane, propane, formaldehyde, methyl ethyl ketone, and lumped >= C3 alkenes). As mentioned in Section 2.3, in the VOC emission inventories, local emission sources in the TP region may be substantially underestimated and the emission trends are not accurately accounted for. Chen et al. (2022) found that emissions of many VOC species in the MEIC inventory were underestimated by about an order of magnitude in Lhasa in 2016. Tang et al. (2022) showed a three-fold increase in the concentrations of aromatic and alkane hydrocarbons in the TP urban areas from 2012-2014 to 2020-2022, which were poorly accounted for in the emission inventories. Given the lack of accurate, timely VOC emission data, we adjust the anthropogenic VOC emissions on the TP in the nested simulations as follows. (1) We multiply emissions by a factor of 10 for the VOC species available in MEIC, and by a factor of 2 for other VOC species available in CEDS but not MEIC. The different scaling choice is based on the fact that for the same VOC species available in both CEDS and MEIC, the emissions in CEDS are 4-6 times greater than MEIC over the TP. (2) For alkanes and aromatics, we further account for the emission trends by using the adjusted 2016 emissions in (1) as the baseline, assuming that emissions increased by a factor of three from 2013 to 2021, and assuming that such emission growth was linear.

We conduct multiple simulations to examine the impacts of emission changes on ozone (Table S1). The BASE scenario simulated ozone concentrations in 2015. The E19, NLE19, and LE19 scenarios are used

to simulate ozone concentrations as a result of changes in emissions of both NO_x and VOCs in different regions. NO_x_E19 and NO_x_NLE19 only changed the NO_x emissions in the corresponding regions."

Table S1: Detailed descriptions of all scenarios are elaborated in Section S1. Here, LE and NLE are abbreviations for 'Local 1.5° Emission' and 'Non-Local Emission', respectively. Meteorology is fixed at the 2015 level.

Scenario	NO_x LE year	VOC LE year	NO_x NLE year	VOC NLE year
BASE	2015	2015	2015	2015
E19	2019	2019	2019	2019
NLE19	2015	2015	2019	2019
LE19	2019	2019	2015	2015
NO_x_E19	2019	2015	2019	2015
NO_x_NLE19	2015	2015	2019	2015

Table S2: Changes in averaged ozone mixing ratios over 2015–2019 simulated by the nested GEOS-Chem model. The results of the averaged ozone mixing ratio change are represented by the mean value and standard deviation of ozone changes in 17 cities.

Factor	Calculation method	Averaged ozone mixing ratio change [ppb]
Emission	E19 minus BASE	1.52±0.51
Non-local emission	NLE19 minus BASE	1.21±0.57
Local emission	LE19 minus BASE	0.71±0.37
NO_x emission	NO_x_E19 minus BASE	1.34±0.61
Non-local NO_x emission	NO_x_NLE19 minus BASE	1.02±0.73

Given the current limitations of CTM model simulations for the TP, we have elected to use the QNR method to analyze the drivers of TP urban ozone changes, and used the CTM simulations to compare with the QNR results as an independent validation. We agree that there are still great challenges in allocating the contributions of multiple factors of ozone change over this unique region (with very small cities, complex terrains and poorly known emissions, etc.). Thus we have further revised the manuscript to better reflect such challenges as well as the uncertainty from the methods taken in our study, as follows.

Lines 179-181:

"The QNR value for a given grid cell represents the amount of NO_x emitted into an air mass passing through its footprint layer, thus serving as a semi-quantitative indicator of ozone transport strength from emission source regions (Cooper et al., 2010; Stohl, 2003)."

Lines 200-215:

"Note that the QNR method does not account for the nonlinearity in ozone chemistry and the impact of

VOC emission changes. Thus, its results should be interpreted as semi-quantitative inference of ozone source contributions. On the other hand, although the CTM explicitly accounts for the effects of chemical nonlinearity and VOC emissions, it is subject to substantial challenges in simulating the TP urban ozone. First, there is no reliable VOC emission dataset for the TP and surrounding areas to allow a full exploration of the role of VOC in ozone growth. Existing bottom-up emission inventories do not or poorly account for local emission sources (e.g., combustion of cow dung and other biofuels used for cooking and/or heating, and incense burning in religious activities) and emission factors, which has been confirmed in many studies (Cui et al., 2018; Lu et al., 2020; Chen et al., 2022; Tang et al., 2022; Li et al., 2023a; Li et al., 2023b), leading to large uncertainties in the calculated magnitude and spatial distribution of VOC emissions. Second, the local topography is complex in the TP (Kong et al., 2022) and the spatial scale of human activities on the TP is small and spatially dispersed, with the built-up area slightly larger than 100 km^2 in Xining and Lhasa and below 30 km^2 in other cities. Proper simulation of ozone chemistry in these cities requires a CTM resolution of 0.05° – 0.1°, for both meteorology and emissions, which poses a great challenge for current-generation CTMs in simulating the whole TP domain and surrounding areas (for local and non-local source attributions). Considering these limitations, we have elected to use the trajectory model and QNR results for ozone source analysis, and further use nested GEOS-Chem CTM simulations to evaluate the impacts of simplification in the QNR method. The configuration of the nested GEOS-Chem model is shown in Supplementary material S1."

Lines 451-471:

"In contrast, the non-local QNR, calculated by combining the HYSPLIT modeling and NO_x emissions for the areas outside 1.5° range of each city, shows a growth rate of 0.14 ppb yr^{-1}. The non-local QNR growth is driven by the changes in the transport pathway of air mass and the anthropogenic emission increases in non-local source regions. This likely suggests a substantial non-local contribution to the observed urban ozone growth over the TP, due to the rapid increase of anthropogenic emissions in the transport source regions and more frequent transport of air masses passing through non-local high-emission regions.

The local QNR for the 17 cities exhibits a growth of 0.06 ppb yr^{-1} (or 33.5% in total) from 2015 and 2019, with the majority caused by the increase in local NO_x emissions (by 31.4%). This is an indication of important contribution of local precursor emissions to the observed TP urban ozone growth. Considering the ozone loss during atmospheric transport at different distances, local and non-local contributions to the rapid rise in the TP urban ozone might be comparable.

Overall, our study suggests that the large rate of urban ozone growth over the TP cities during the recent decade is likely caused by a combination of increases in local anthropogenic emissions, non-local anthropogenic emissions and more frequent transport passing through non-local high-emission regions. These local and non-local factors should be considered in future studies of ozone and its mitigation over the plateau.

It is important to note that the QNR does not consider the nonlinearity in ozone chemistry and VOC emissions, which may introduce uncertainty in ozone source attribution. Although the QNR results are supported by nested GEOS-Chem CTM simulations for summertime ozone, the CTM simulations themselves are subject to limitations in resolution and emission inputs. Future work should focus on obtaining reliable, high-resolution precursor emissions, especially for speciated VOC emissions. Combining the trajectory models, CTMs and statistical and/or artificial intelligence methods might allow for low-cost kilometer-resolution simulation of ozone chemistry and source inference to better quantify

the individual and combined effects of various emission and meteorological factors on the TP urban ozone."

In addition, to further improve our calculations, we have updated to the latest version of the PHLET-OMI emissions for NO_x. We updated the process of removing the contributions of natural emission sources (soil and open fire) to focus on anthropogenic influences. We used soil microbial emissions (Weng et al., 2020) and open fire emissions from the Global Fire Emissions Database (GFED4, last access: Dec/08/2022; Giglio et al. (2013)) that incorporate inter-annual variability rather than fixed emissions (Kong, H., personal communication, March 12, 2025). This update improved the accuracy of anthropogenic emission trends. It has a minor effect on some of the QNR trend estimates and does not change the main conclusions. The associated updates in the main text are as follows:

Line 22-24:

Old: "Non-local factors contribute positively to the urban ozone trends, due mainly to more frequent transport passing through the footprint layers (0–300 m above the ground) of non-local high-emission regions. Another important contributor to the urban ozone growth is the 26.5% increase in local anthropogenic NO_x emissions."

New: "Non-local factors contribute to the urban ozone growth, due to increased anthropogenic emissions in non-local source regions and changes in transport pathways. Another important contributor to the urban ozone growth is the 31.4% increase in local anthropogenic NO_x emissions."

Lines 218-231:

Old: "Thus, for the back-trajectory calculations, we use top-down NOx emission data to reduce the effect of emission errors. The top-down NOx emission data are from PHLET-OMI (Kong et al., 2022; Kong et al., 2019), which estimates June–August average NOx emissions at 0.05° × 0.05° in Asia (15°-55° N, 70°-140° E; Fig. 1a). PHLET-OMI is obtained by employing the POMINO-OMI satellite product for tropospheric NO2 vertical column densities (VCDs) (Liu et al., 2019; Lin et al., 2015a; Lin et al., 2014) and the PHLET algorithm for emission retrieval. The PHLET emission data reveal considerable amounts of emission sources unaccounted in existing bottom-up anthropogenic emission inventories (Kong et al., 2022) and natural emission parametrization (Kong et al., 2023). For example, the provincial total anthropogenic emissions of Tibet in PHLET are higher than current inventories by 3 to 7 times (Kong et al., 2022). PHLET-OMI provides June–August average NOx emissions in each year from 2012 to 2020. We remove the contributions of natural emission sources to focus on anthropogenic influences, following the method by Kong et al. (2022)."

New: "Thus, for the back-trajectory calculations, we use top-down NO_x emission data to reduce the effect of emission errors. The top-down NO_x emission data are an updated version of PHLET-OMI (Kong et al., 2022; Kong et al., 2019; Kong et al., 2025), which estimates June–August average NO_x emissions at 0.05° × 0.05° in Asia (15°-55° N, 70°-140° E; Fig. 1a). PHLET-OMI is obtained by employing the POMINO-OMI satellite product for tropospheric NO_2 vertical column densities (VCDs) (Liu et al., 2019; Lin et al., 2015; Lin et al., 2014) and the PHLET algorithm for emission retrieval. The PHLET emission data reveal considerable amounts of emission sources unaccounted in existing bottom-up anthropogenic emission inventories (Kong et al., 2022) and natural emission parametrization (Kong et al., 2023). For example, the provincial total anthropogenic emissions of Tibet in PHLET are higher than current

inventories by 3 to 7 times (Kong et al., 2022); this result is confirmed by recent emission inference based on near-surface measurements (Zhang et al., 2025).

PHLET-OMI provides June–August average NO_x emissions in each year from 2012 to 2020. We remove the contributions of natural emission sources (soil and open fire) to focus on anthropogenic influences. We employ soil microbial emissions (Weng et al., 2020) and open fire emissions from the Global Fire Emissions Database (GFED4, last access: Dec/08/2022; Giglio et al. (2013)) that incorporate inter-annual variability (Kong et al., 2025)."

Lines 354-358:

Old: "From 2015 to 2019, the non-local QNR increases at a rate of 0.11 ppb yr^{-1} (p-value = 0.16) (Fig. 7a). The QNR growth rate due to changes in transport pathway alone is about 0.10 ppb yr^{-1} (p-value = 0.15), while emission changes alone result in little trend of QNR (Fig. 7b-c). The non-local QNR is mainly driven by changes in South Asia (India, Bangladesh, etc.) and the central and western provinces of China (Sichuan, Gansu, etc.)."

New: "From 2015 to 2019, the non-local QNR increases at a rate of 0.14 ppb yr^{-1} (p-value = 0.04) (Fig. 7a). The QNR growth rate due to changes in transport pathway alone is about 0.07 ppb yr^{-1} (p-value = 0.20), while emission changes alone result in a trend of 0.06 ppb yr^{-1} (p-value = 0.00) (Fig. 7b-c). The non-local QNR is mainly driven by changes in South Asia (India, Bangladesh, etc.) and the central and western provinces of China (Gansu, Sichuan, etc.)."

Lines 378-381:

Old: "The interannual variation of QNR for the Waliguan background station is similar to that for the MEE stations (Fig. S6). These results suggest a considerable positive contribution of regional transport to ozone growth over the whole plateau."

New: "The interannual variation of non-local QNR for the Waliguan background station is similar to that for the MEE stations, although with a stronger contribution from transport pathway and a weaker contribution from non-local emission changes (Fig. S6a-c). These results suggest a considerable positive contribution of regional transport to ozone growth over the whole plateau."

Lines 384-386:

Old: "The interannual variation of three-year summer average local NO_x emissions show a growth of 26.5% from 1.81 tons h^{-1} in 2015 to 2.29 tons h^{-1} in 2019 (Fig. 8a)."

New: "The interannual variation of three-year summer average local anthropogenic NO_x emissions show a growth of 31.4% from 1.49 tons h^{-1} in 2015 to 1.96 tons h^{-1} in 2019 (Fig. 8a)."

Lines 407-413:

Old: "Figure 8b further shows that for the 17 cities, the local contribution to QNR increases significantly from 2015 to 2019 with a trend of 0.05 ppb yr^{-1}, with a total growth of 23% over these years. This trend is contributed mainly by the growth in local NO_x emissions (26.5%). It contrasts with the respective trend of local QNR for Waliguan (-0.07ppb yr^{-1}) (Fig. S6d). The local QNR growth for the 17 cities (0.05 ppb yr^{-1}) is smaller than that for the non-local contribution (0.11 ppb yr^{-1}, Fig. 7a). We further analyzed the average QNR for the three cities with decreasing trends. As shown in Fig. S7, the trend of non-local contributions is slightly smaller than the average of the other cities on the TP, while the local

contributions show a decreasing trend (-0.02 ppb yr^{-1})."

New: "Figure 8b further shows that for the 17 cities, the local contribution to QNR increases significantly from 2015 to 2019 with a trend of 0.06 ppb yr-1, with a total growth of 33.5% over these years. This trend is contributed mainly by the growth in local NOx emissions (31.4%). It contrasts with the respective trend of local QNR for Waliguan (-0.00 ppb yr-1) (Fig. S6d). The local QNR growth for the 17 cities (0.06 ppb yr-1) is smaller than that for the non-local contribution (0.14 ppb yr-1, Fig. 7a). We further analyzed the average QNR for the three cities with decreasing trends (Lhasa, Changdu and Hainan). As shown in Fig. S7, the trend of non-local contributions is slightly higher than the average of the other cities on the TP, while the local contributions show a weak decreasing trend (-0.01 ppb yr^{-1})."

Lines 451-460:

Old: "In contrast, the non-local QNR, calculated by combining the HYSPLIT modeling and NO_x emissions for the areas outside 1.5° range of each city, exhibits a growth rate of 0.11 ppb yr^{-1}. This suggests a substantial non-local contribution to the urban ozone trends. The non-local contribution is due mainly to the changes in transport pathway of air mass rather than the changes in anthropogenic emissions. This means that the growth of urban ozone over the TP may be related to more frequent transport of air masses passing through non-local high-emission regions.

The local QNR for the 17 cities exhibits a growth of 0.05 ppb yr^{-1} (or 23% in total) from 2015 and 2019, with the majority caused by the increase in local NO_x emissions (by 26.5%). Considering the ozone loss during atmospheric transport at different distances, local and non-local contributions to the rapid rise in the TP urban ozone might be comparable."

New: "In contrast, the non-local QNR, calculated by combining the HYSPLIT modeling and NO_x emissions for the areas outside 1.5° range of each city, shows a growth rate of 0.14 ppb yr^{-1}. The non-local QNR growth is driven by the changes in the transport pathway of air mass and the anthropogenic emission increases in non-local source regions. This likely suggests a substantial non-local contribution to the observed urban ozone growth over the TP, due to the rapid increase of anthropogenic emissions in the transport source regions and more frequent transport of air masses passing through non-local high-emission regions.

The local QNR for the 17 cities exhibits a growth of 0.06 ppb yr^{-1} (or 33.5% in total) from 2015 and 2019, with the majority caused by the increase in local NO_x emissions (by 31.4%). This is an indication of important contribution of local precursor emissions to the observed TP urban ozone growth. Considering the ozone loss during atmospheric transport at different distances, local and non-local contributions to the rapid rise in the TP urban ozone might be comparable."

Figure 7

Old:

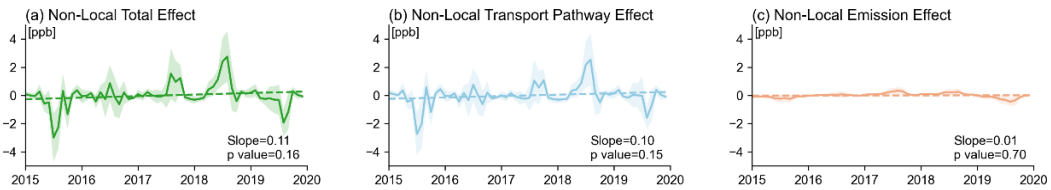

Figure 7 Deseasonalized monthly variation of non-local QNR averaged over the 17 cities. (a) Non-local QNR changes due to the combined effect of changes in anthropogenic emissions and in transport pathway. (b) Non-

local QNR changes due to transport pathway alone. (c) Non-local QNR changes due to anthropogenic emissions alone. The shaded area represents the standard deviation of the data across 17 cities.

New:

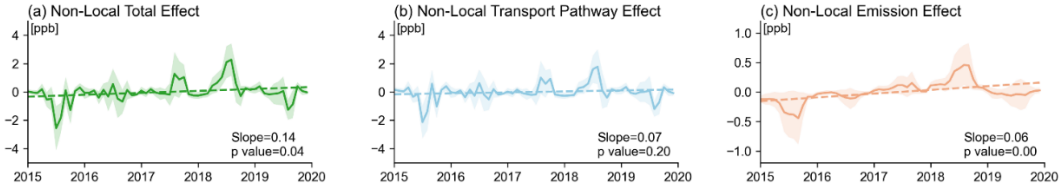

Figure 7 Deseasonalized monthly variation of non-local QNR averaged over the 17 cities. (a) Non-local QNR changes due to the combined effect of changes in anthropogenic emissions and in transport pathway. (b) Non-local QNR changes due to transport pathway alone. (c) Non-local QNR changes due to anthropogenic emissions alone. The shaded area represents the standard deviation of the data across 17 cities.

Figure 8

Old:

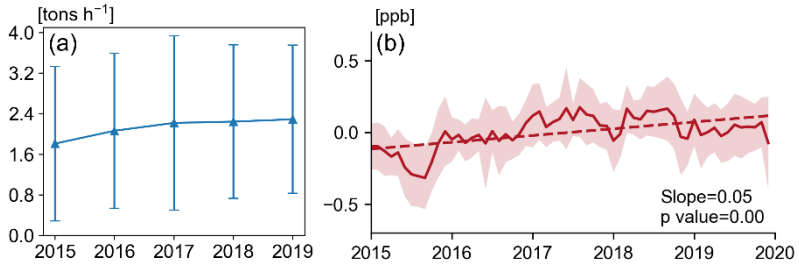

Figure 8 Changes in local anthropogenic emissions and QNR for within 1.5° of the 17 cities. (a) Time series of three-year moving average PHLET-OMI NO_x anthropogenic emissions in summer. Here, the value for 2015 represents the average over 2014–2016, and so on. (b) Deseasonalized monthly variation of local QNR. The error bar in (a) and shaded area in (b) represent the standard deviation of data across 17 cities.

New:

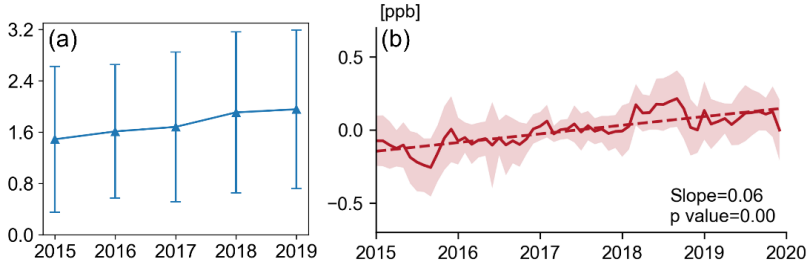

Figure 8 Changes in local anthropogenic emissions and QNR for within 1.5° of the 17 cities. (a) Time series of three-year moving average PHLET-OMI NO_x anthropogenic emissions in summer. Here, the value for 2015 represents the average over 2014–2016, and so on. (b) Deseasonalized monthly variation of local QNR. The error bar in (a) and shaded area in (b) represent the standard deviation of data across 17 cities.

Figure S5

Old:

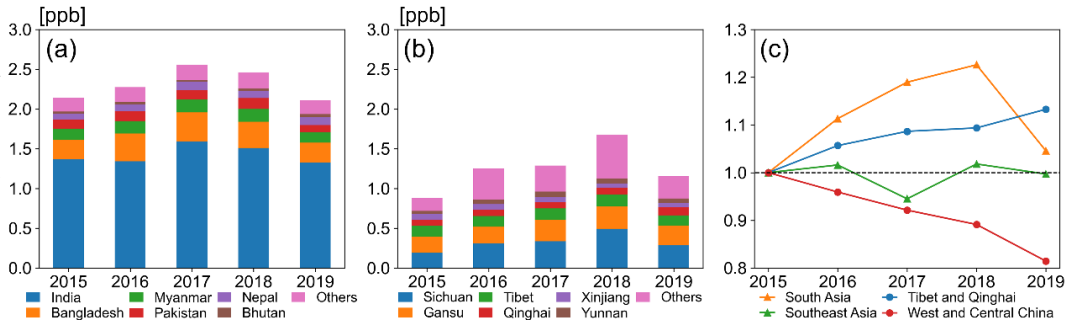

Figure S5 Annual variation of non-local QNR over 17 cities from (a) foreign countries and (b) provinces of China. Each of the five provinces or countries with the largest average QNR contribution in 2015 is marked with a separate color. (c) Normalized time series of three-year moving average PHLET-OMI NOx anthropogenic emissions in summer for different regions, with summer 2015 emissions as a baseline. Here, the value for 2015 represents the average over 2014–2016, and so on. South Asia includes India, Maldives, Bhutan, Sri Lanka, Pakistan, Bangladesh and Nepal; Southeast Asia includes Philippines, Vietnam, Laos, Cambodia, Myanmar, Thailand, Malaysia, Brunei Darussalam, Singapore, Indonesia, Timor-Leste; and West and Central China includes Inner-Mongolia, Guangxi, Chongqing, Sichuan, Guizhou, Yunnan, Shaanxi, Gansu, Ningxia, Xinjiang, Shanxi, Anhui, Jiangxi, Henan, Hubei, Hunan.

New:

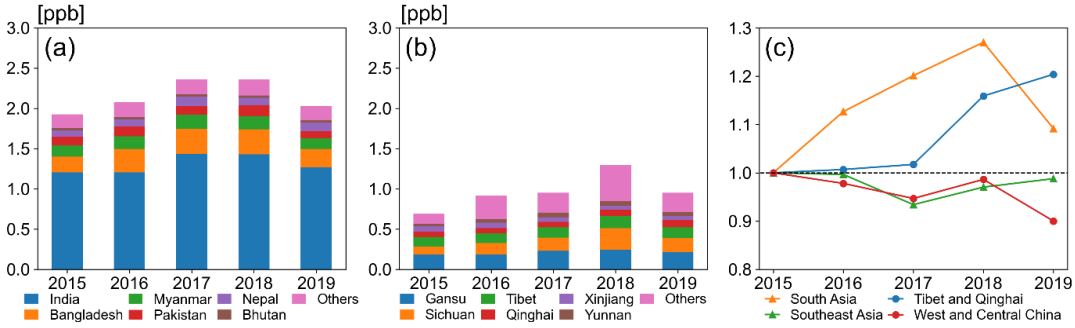

Figure S5 Annual variation of non-local QNR over 17 cities from (a) foreign countries and (b) provinces of China. Each of the five provinces or countries with the largest average QNR contribution in 2015 is marked with a separate color. (c) Normalized time series of three-year moving average PHLET-OMI NOx anthropogenic emissions in summer for different regions, with summer 2015 emissions as a baseline. Here, the value for 2015 represents the average over 2014–2016, and so on. South Asia includes India, Maldives, Bhutan, Sri Lanka, Pakistan, Bangladesh and Nepal; Southeast Asia includes Philippines, Vietnam, Laos, Cambodia, Myanmar, Thailand, Malaysia, Brunei Darussalam, Singapore, Indonesia, Timor-Leste; and West and Central China includes Inner-Mongolia, Guangxi, Chongqing, Sichuan, Guizhou, Yunnan, Shaanxi, Gansu, Ningxia, Xinjiang, Shanxi, Anhui, Jiangxi, Henan, Hubei, Hunan.

Figure S6

Old:

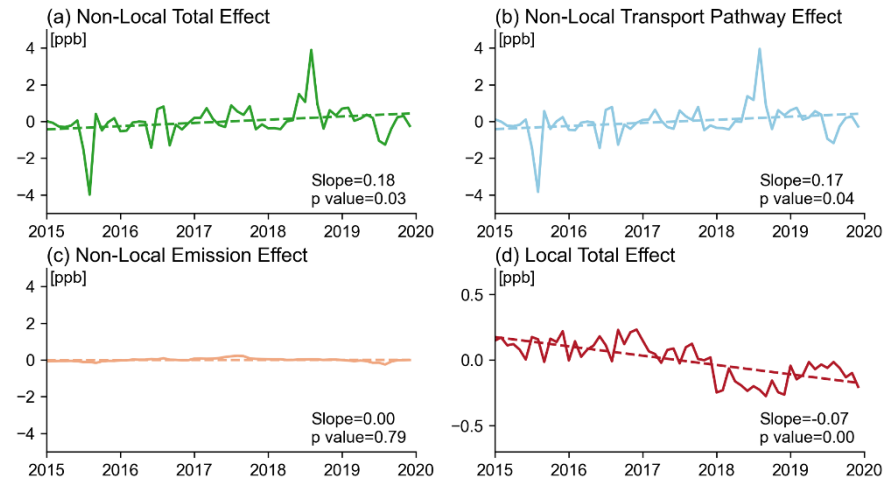

Figure S6 Deseasonalized monthly variation of QNR at Waliguan. (a) Non-local QNR changes due to the combined effect of changes in anthropogenic emissions and in transport pathway. (b) Non-local QNR changes due to changes in transport pathway alone. (c) Non-local QNR changes due to changes in anthropogenic emissions alone. (d) Local QNR changes due to the combined effect of changes in anthropogenic emissions and in transport pathway.

New:

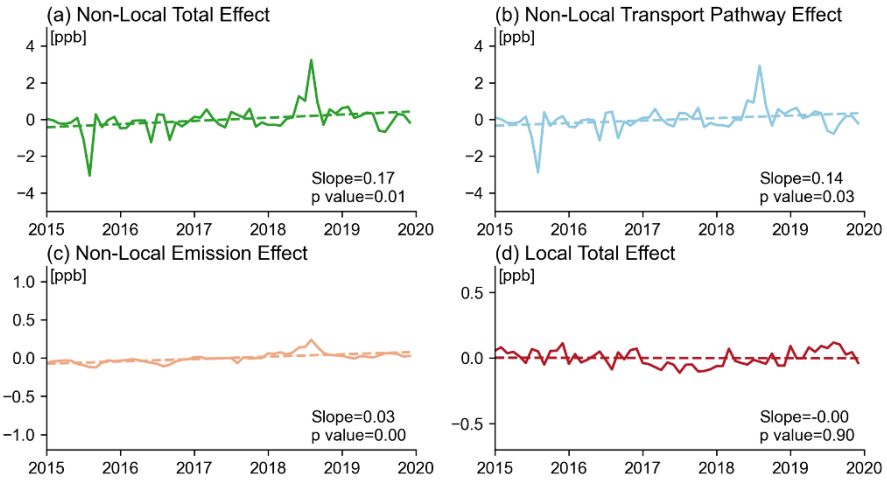

Figure S6 Deseasonalized monthly variation of QNR at Waliguan. (a) Non-local QNR changes due to the combined effect of changes in anthropogenic emissions and in transport pathway. (b) Non-local QNR changes due to changes in transport pathway alone. (c) Non-local QNR changes due to changes in anthropogenic emissions alone. (d) Local QNR changes due to the combined effect of changes in anthropogenic emissions and in transport pathway.

Figure S7

Old:

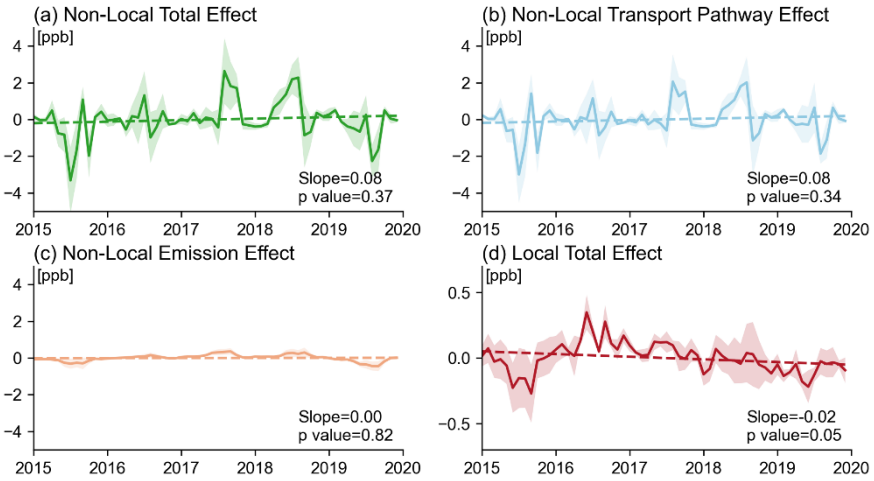

Figure S7 Deseasonalized monthly variation of QNR over 3 cities (Changdu, Hainan and Lhasa). (a) Non-local QNR changes due to the combined effect of changes in anthropogenic emissions and in transport pathway. (b) Non-local QNR changes due to changes in transport pathway alone. (c) Non-local QNR changes due to changes in anthropogenic emissions alone. (d) Local QNR changes due to the combined effect of changes in anthropogenic emissions and in transport pathway.

New:

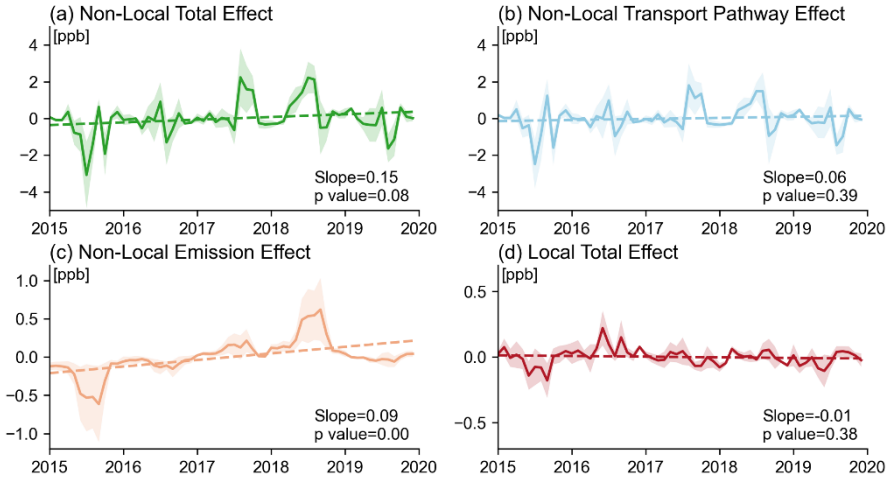

Figure S7 Deseasonalized monthly variation of QNR over 3 cities (Changdu, Hainan and Lhasa). (a) Non-local QNR changes due to the combined effect of changes in anthropogenic emissions and in transport pathway. (b) Non-local QNR changes due to changes in transport pathway alone. (c) Non-local QNR changes due to changes in anthropogenic emissions alone. (d) Local QNR changes due to the combined effect of changes in anthropogenic emissions and in transport pathway.

Reference

Chen, S., Wang, W., Li, M., Mao, J., Ma, N., Liu, J., Bai, Z., Zhou, L., Wang, X., Bian, J., and Yu, P.: The Contribution of Local Anthropogenic Emissions to Air Pollutants in Lhasa on the Tibetan Plateau, Journal of Geophysical Research: Atmospheres, 127, 10.1029/2021jd036202, 2022.

Cooper, O. R., Parrish, D. D., Stohl, A., Trainer, M., Nédélec, P., Thouret, V., Cammas, J. P., Oltmans, S. J., Johnson, B. J., Tarasick, D., Leblanc, T., McDermid, I. S., Jaffe, D., Gao, R., Stith, J., Ryerson, T., Aikin, K., Campos, T., Weinheimer, A., and Avery, M. A.: Increasing springtime ozone mixing ratios in the free troposphere over western North America, Nature, 463, 344-348, 10.1038/nature08708, 2010.

Cui, Y. Y., Liu, S., Bai, Z., Bian, J., Li, D., Fan, K., McKeen, S. A., Watts, L. A., Ciciora, S. J., and Gao, R.-S.: Religious burning as a potential major source of atmospheric fine aerosols in summertime Lhasa on the Tibetan Plateau, Atmospheric Environment, 181, 186-191, https://doi.org/10.1016/j.atmosenv.2018.03.025, 2018.

Giglio, L., Randerson, J. T., and van der Werf, G. R.: Analysis of daily, monthly, and annual burned area using the fourth-generation global fire emissions database (GFED4), 118, 317-328, https://doi.org/10.1002/jgrg.20042, 2013.

Kong, H., Lin, J., Chen, L., Zhang, Y., Yan, Y., Liu, M., Ni, R., Liu, Z., and Weng, H.: Considerable Unaccounted Local Sources of NO(x) Emissions in China Revealed from Satellite, Environmental Science & Technology, 56, 7131-7142, 10.1021/acs.est.1c07723, 2022.

Kong, H., Lin, J., Ni, R., Du, M., Wang, J., Chen, L., Xu, C., Yan, Y., Weng, H., and Zhang, Y.: Satellite Detected Weak Decline of Nitrogen Oxides Emissions in Economically Small Cities of China, submitted to Environmental Research Letters, 2025.

Kong, H., Lin, J., Zhang, R., Liu, M., Weng, H., Ni, R., Chen, L., Wang, J., Yan, Y., and Zhang, Q.: High-resolution (0.05° × 0.05°) NOx emissions in the Yangtze River Delta inferred from OMI, Atmospheric Chemistry and Physics, 19, 12835-12856, 10.5194/acp-19-12835-2019, 2019.

Kong, H., Lin, J., Zhang, Y., Li, C., Xu, C., Shen, L., Liu, X., Yang, K., Su, H., and Xu, W.: High natural nitric oxide emissions from lakes on Tibetan Plateau under rapid warming, Nature Geoscience, 16, 474-477, 10.1038/s41561-023-01200-8, 2023.

Li, M., Liu, H., Geng, G., Hong, C., Liu, F., Song, Y., Tong, D., Zheng, B., Cui, H., Man, H., Zhang, Q., and He, K.: Anthropogenic emission inventories in China: a review, National Science Review, 4, 834-866, 10.1093/nsr/nwx150, 2017.

Li, Q., Gong, D., Wang, H., Deng, S., Zhang, C., Mo, X., Chen, J., and Wang, B.: Tibetan Plateau is vulnerable to aromatic-related photochemical pollution and health threats: A case study in Lhasa, Science of The Total Environment, 904, 166494, https://doi.org/10.1016/j.scitotenv.2023.166494, 2023a.

Li, W., Han, X., Li, J., Lun, X., and Zhang, M.: Assessment of surface ozone production in Qinghai, China with satellite-constrained VOCs and NOx emissions, Science of The Total Environment, 905, 166602, https://doi.org/10.1016/j.scitotenv.2023.166602, 2023b.

Lin, J. T., Liu, M. Y., Xin, J. Y., Boersma, K. F., Spurr, R., Martin, R., and Zhang, Q.: Influence of aerosols and surface reflectance on satellite NO2 retrieval: seasonal and spatial characteristics and implications for NOx emission constraints, Atmospheric Chemistry and Physics, 15, 11217-11241, 10.5194/acp-15-11217-2015, 2015.

Lin, J. T., Martin, R. V., Boersma, K. F., Sneep, M., Stammes, P., Spurr, R., Wang, P., Van Roozendael, M., Clémer, K., and Irie, H.: Retrieving tropospheric nitrogen dioxide from the Ozone Monitoring Instrument: effects of aerosols, surface reflectance anisotropy, and vertical profile of nitrogen dioxide, Atmospheric Chemistry and Physics, 14, 1441-1461, 10.5194/acp-14-1441-2014, 2014.

Liu, M., Lin, J., Boersma, K. F., Pinardi, G., Wang, Y., Chimot, J., Wagner, T., Xie, P., Eskes, H., Van Roozendael, M., Hendrick, F., Wang, P., Wang, T., Yan, Y., Chen, L., and Ni, R.: Improved aerosol correction for OMI tropospheric NO₂ retrieval over East Asia: constraint from CALIOP aerosol vertical profile, Atmospheric Measurement Techniques, 12, 1-21, 10.5194/amt-12-1-2019, 2019.

Lu, F., Li, S., Shen, B., Zhang, J., Liu, L., Shen, X., and Zhao, R.: The emission characteristic of VOCs and the toxicity of BTEX from different mosquito-repellent incenses, Journal of Hazardous Materials, 384, 121428, https://doi.org/10.1016/j.jhazmat.2019.121428, 2020.

Stohl, A.: A backward modeling study of intercontinental pollution transport using aircraft measurements, Journal of Geophysical Research, 108, 10.1029/2002jd002862, 2003.

Tang, G., Yao, D., Kang, Y., Liu, Y., Liu, Y., Wang, Y., Bai, Z., Sun, J., Cong, Z., Xin, J., Liu, Z., Zhu, Z., Geng, Y., Wang, L., Li, T., Li, X., Bian, J., and Wang, Y.: The urgent need to control volatile organic compound pollution over the Qinghai-Tibet Plateau, iScience, 25, 105688, https://doi.org/10.1016/j.isci.2022.105688, 2022.

Weng, H., Lin, J., Martin, R., Millet, D. B., Jaeglé, L., Ridley, D., Keller, C., Li, C., Du, M., and Meng, J.: Global high-resolution emissions of soil NOx, sea salt aerosols, and biogenic volatile organic compounds, Scientific Data, 7, 148, 10.1038/s41597-020-0488-5, 2020.

Zhang, M., Wang, S., Yu, W., Tao, C., Zhu, S., Ma, J., Wang, P., and Zhang, H.: The Major Role of Anthropogenic Emission Underestimation in PM2.5 Estimation Uncertainty Over the Tibetan Plateau, 52, e2024GL110513, https://doi.org/10.1029/2024GL110513, 2025.

Zheng, B., Tong, D., Li, M., Liu, F., Hong, C., Geng, G., Li, H., Li, X., Peng, L., Qi, J., Yan, L., Zhang, Y., Zhao, H., Zheng, Y., He, K., and Zhang, Q.: Trends in China's anthropogenic emissions since 2010 as the consequence of clean air actions, Atmospheric Chemistry and Physics, 18, 14095-14111, 10.5194/acp-18-14095-2018, 2018.